Environmental Pollution 190 (2014) 91–100

Contents lists available at ScienceDirect

Environmental Pollution

journal homepage: www.elsevier.com/locate/envpol

Decomposing the profile of PM in two low polluted German cities – Mapping of air mass residence time, focusing on potential long range transport impacts

Konstantinos Dimitriou, Pavlos Kassomenos*

Laboratory of Meteorology, Department of Physics, University of Ioannina, 45110 Ioannina, Greece

ARTICLE INFO

Article history:
Received 28 January 2014
Received in revised form
11 March 2014
Accepted 13 March 2014
Available online 15 April 2014

Keywords:
PM_{10}
$PM_{2.5}$
Air mass trajectories
Cluster analysis
Residence time
Germany
Air quality

ABSTRACT

This paper aims to decompose the profile of particulates in Karlsruhe and Potsdam (Germany), focusing on the localization of PM potential transboundary sources. An air mass cluster analysis was implemented, followed by a study of air mass residence time on a grid of a $0.5^\circ \times 0.5^\circ$ resolution. Particulate/gaseous daily air pollution and meteorological data were used to indicate PM local sources. Four Principal Component Analysis (PCA) components were produced: traffic, photochemical, industrial/domestic and particulate. $PM_{2.5}/PM_{10}$ ratio seasonal trends, indicated production of PM_{COARSE} (PM_{10}–$PM_{2.5}$) from secondary sources in Potsdam during warm period (WP). The residing areas of incoming slow moving air masses are potential transboundary PM sources. For Karlsruhe those areas were mainly around the city. An air mass residence time secondary peak was observed over Stuttgart. For Potsdam, areas with increased dwelling time of the arriving air parcels were detected particularly above E/SE Germany.

1. Introduction

Human exposure to outdoor air pollution is associated with adverse health effects (Chen et al., 2010). Elevated concentrations of PM_{10} (diameter less than 10 um) and primarily $PM_{2.5}$ (diameter less than 2.5 um) particulate matter (Linares and Diaz, 2010), are related with increased respiratory and cardiovascular incidents (Guo et al., 2010; Jiménez et al., 2010), mainly within the most vulnerable cohorts of the population (Tabaku et al., 2011, Jiménez et al., 2009). European Union (EU) legislation has set the daily limit for PM_{10} at 50 ugr/m^3, an average concentration that should not be exceeded more than 35 times per year, whereas the annual limit is set at 40 ugr/m^3. For $PM_{2.5}$ only an annual EU limit of 25 ugr/m^3 is established. Various local and transboundary sources of particulates (Viana et al., 2014; Kuo et al., 2014; Mirante et al., 2014) affect air quality in urban areas.

Principal Component Analysis (PCA) is a commonly used technique for the identification of the origin of air pollutants (Sarkar and Khillare, 2013; Zhu et al., 2013). High loadings of gaseous pollutants in PCA components have been used as markers of local emission sources (Dimitriou and Kassomenos, 2013; Yoo et al., 2011; Vardoulakis and Kassomenos, 2008). PCA identified four factors of air pollution in Modena and three in Castello (Minguillon et al., 2013).

Backward atmospheric trajectories are implemented to identify intrusions of exogenous PM in urban areas (Riccio et al., 2007). The classification scheme of backward trajectories, defined three aerosol types enriching the atmosphere of Gdynia in Poland (Lewandowska et al., 2013), and indicated long range transport of PM in East Hungary, from the so called "Black triangle" region of Central Europe (Borbely-Kiss et al., 1999). Slow moving short range trajectories were associated with higher concentrations of PM (Makra et al., 2011; Kassomenos et al., 2012), due to increased residence time of air parcels over potential source areas (Salvador et al., 2010; Karaca and Camci, 2010; Fleming et al., 2012).

The residing time of air masses over specific areas, was analyzed by Xu et al. (2006), within a $1^\circ \times 1^\circ$ resolution grid. Multiple-linear regression of the residence time, against the corresponding concentrations at the receptor, was proven to be a useful tool for attributing aerosol loading to relatively large source areas. A similar method was followed by Kavouras et al. (2013), in Amsterdam, Athens, Birmingham and Helsinki, and also by Chalbot et al. (2013),

* Corresponding author.
E-mail addresses: pkassom@uoi.gr, kassomenos.pavlos@gmail.com (P. Kassomenos).

http://dx.doi.org/10.1016/j.envpol.2014.03.019
0269-7491/

Table 1
Information for the Background Environmental (ENVI) and meteorological (METE) monitoring stations in Karlsruhe and Potsdam.

City	Station code and name	Type	Area	Longitude	Latitude
Karlsruhe	DEBW081 (Karlsruhe-Nordwest)	ENVI	Suburban	8.355.556	49.028.610
	0051 (Karlsruhe)	METE		8.210.540	49.020.210
Potsdam	DEBB021 (Potsdam-Zentrum)	ENVI	Urban	13.063.889	52.401.943
	0054 (Potsdam)	METE		13.030.500	52.230.000

to identify and quantify the types of PM_{10} and $PM_{2.5}$ sources in Athens. Polissar et al. (2001) and Kong et al. (2013), implemented a potential PM source contribution function, based on residence time of air masses into the cells of a 0.5° × 0.5° resolution grid.

In this paper, a mixture of statistical techniques is used, in order to decompose the profile of PM in two low polluted German cities namely: Karlsruhe and Potsdam, emphasizing on potential long range transport impacts. Backward atmospheric trajectories corresponding to days with increased PM_{10} concentrations were deployed and organized in clusters at 1500 m and 750 m AGL. Residing time of air masses suspicious for PM long range transport, was analyzed on a 0.5° × 0.5° resolution grid and plotted on density maps, in order to reveal potential transboundary sources of exogenous particulates. PM_{10}, $PM_{2.5}$, NO_2, SO_2, CO and O_3 daily air pollution data, were also elaborated by a PCA analysis during cold (CP) and warm (WP) periods, as to indicate local sources of particulates. In addition, meteorological parameters and $PM_{2.5}/PM_{10}$ fraction values were also studied, in order to support the findings from the other procedures.

2. Data and methodology

2.1. Stations and sampling methods

For this paper, daily (due to the absence of hourly) concentrations of PM_{10} and $PM_{2.5}$ and hourly concentrations of NO_2, SO_2, CO and O_3, measured from one environmental station in Potsdam [DEBB021 "Potsdam-Zentrum"] and one in Karlsruhe [DEBW081 "Karlsruhe-Nodrwest"] (Table 1), were downloaded from the website of the EU Air Quality Database (Airbase) in ugr/m^3 except of CO (mgr/m^3). The range of the dataset has duration of 5 years and extends through the time interval 2003–2007. For the monitoring of $PM_{2.5}$ and PM_{10} concentrations, Gravimetric samplers were used. Analyzers based on UV absorption, UV fluorescence, infrared absorption and Chemiluminescence were used for the measurements of O_3, SO_2, CO and NO_2 respectively. As demanded from EU guidelines, air pollution analysers should operate within 15% of uncertainty bounds. Both of the sampling sites have background characteristics, present low levels of air pollution (Norra and Stuben, 2004), and were selected for this paper because their position facilitates the identification of PM long range transport impacts. In addition, the authors chose DEBB021 and DEBW081 stations, due to the availability of $PM_{2.5}$ data. Average daily mean levels of air pollution at the two sampling sites are separately included in Table 2 for CP [1 October–31 March] and WP [1 April–30 September] (Dimitriou and Kassomenos, 2013). The role of meteorology was also taken into account for this paper, thus daily Mean Wind Speed (MWS in m/s), daily Maximum Wind Gust (MWG in m/s) and daily Relative Humidity (RH in 1%) data, were elaborated at a daily base. These meteorological data were produced by in situ measurements performed by one meteorological station in Karlsruhe [0051 "Karlsruhe"] and one in Potsdam [0054 "Potsdam"] (Table 1), and were downloaded from the website of the European Climate Assessment & Dataset project (ECA&D). Hourly values of meteorological parameters were not available in the database.

2.2. Description of sampling sites

2.2.1. Karlsruhe

The city of Karlsruhe belongs to the German state of Baden-Württemberg, in southwest Germany, and has a population of approximately 300,000 inhabitants. Background air pollution monitoring station Karlsruhe-Nordwest (DEBW081) is localized at the north western part of the city of Karlsruhe. The sampling site's area is mainly industrial and secondarily residential. The station is sited at a parking site across the railway lines, neighboring to the two line road of "Daimler Strasse". The nearest major street to the sampling site is "Neureuter Strasse", but the traffic flow has no direct impact at the station's measurements. High buildings exist within a 100 m radius around the station's position and the remaining land between them is covered by lawn (Norra and Stuben, 2004), but generally the vegetation is very limited with no high trees and bushes. In addition, the coal fired thermal plant "Rheinhafen" (longitude: 49.012.568, latitude: 8.302.000), situated 2 km southwest of the Karlsruhe-Nordwest station, is a major source of air pollution which has to be underlined, while the oil refinery "Oberrhein" (longitude = 8.329.880, latitude = 49.058.950), is also located 3.5 km to the north away from the sampling site.

2.2.2. Potsdam

The city of Potsdam is the capital city of the German state of Brandenburg, has a total population of approximately 160,000 people, and is located 26 km to the west of the city of Berlin, the capital of Germany. Background air pollution monitoring station Potsdam-Zentrum (DEBB021) is sited at the northwest part of a city block located in the center of Potsdam. This city block is surrounded by a network of four streets namely: "Hebbel Strasse", "Gutenberg Strasse", "Am Bassin" and "Charlotten Strasse", and principally includes the "Bassiinplatz" park and a parking space. No high buildings and no important industrial units exist in the vicinity of the sampling site, whereas the area around the block is mainly residential. The nearby wide street of "Gutenberg Strasse" has no direct

Table 2
Average daily mean concentration values of PM_{10}, $PM_{2.5}$, NO_2, SO_2, CO and O_3 at DEBB021 and DEBW081 during cold [CP] and warm [WP] seasons separately.

Station	Period	$PM_{2.5}$ (ug/m^3)	PM_{10} (ug/m^3)	SO_2 (ug/m^3)	O_3 (ug/m^3)	CO (mg/m^3)	NO_2 (ug/m^3)
DEBW081	CP	20.17	26.12	7.29	29.50	0.31	30.10
	WP	11.46	17.09	3.76	62.40	0.16	17.80
DEBB021	CP	21.31	28.53	5.02	34.10	0.54	28.00
	WP	13.19	21.40	3.41	67.80	0.36	18.90

influence at the station's measurements, due to the station's position away from the road curbs. The "Bassiinplatz" park, which is neighboring to the Potsdam-Zentrum station, contains trees and bushes, and the soil is covered with grass.

2.3. Methodology

A PCA analysis was implemented, in order to define components corresponding to local sources of air pollution (Yoo et al., 2011; Vardoulakis and Kassomenos, 2008). Gaseous air pollutants were used as markers of emission sources. More specifically CO, SO_2 and O_3, were considered as indicators of traffic, industrial, and photochemical air pollution respectively (Deacon et al., 1997), whereas NO_2 is produced by multiple combustion sources. PCA was performed with average daily concentrations of PM_{10}, $PM_{2.5}$, NO_2, SO_2, CO and O_3, due to the lack of hourly data for PM. The availability of at least 18 of each day's 24 hourly concentration values was set as a precondition, in order to be averaged then to daily values. Timelines were divided to cold and warm periods [CP, WP respectively] (Vardoulakis and Kassomenos, 2008), because different climatological conditions and social activities among CP and WP, influence decisively the emission and detection of air pollutants. The fraction $PM_{2.5}/PM_{10}$ was also calculated in a daily basis, to identify possible seasonal changes of PM size distribution among CP and WP (Chaloulakou et al., 2003). An Independent Variables *T*-Test was applied, in order to detect possible statistically significant at 95% Confidence Interval (CI) trends in the proportion of fine particles in the total PM_{10} mass, between CP and WP (Gehrig and Buchmann, 2003). Pearson Correlation Coefficients (PCC) were also calculated among meteorological factors (MWS, MWG and RH) and daily mean concentrations of PM_{10} (Demirci and Cuhadaroglou, 2000; Oguz et al., 2003; Gupta et al., 2004), as to reveal possible statistically significant correlations.

HYSPLIT trajectory model of the NOAA Air Resources Laboratory was used, in order to define atmospheric pathways, possibly contributing to elevated PM_{10} concentrations (Karaca et al., 2009; Riccio et al., 2007) due to long range transport, in Karlsruhe and Potsdam. A five year period (2003–2007) was studied. During this period, 10% of days with highest daily PM_{10} concentrations were used as temporal starting points for the extraction of 4-day backward air mass trajectories (Charron et al., 2007; Grivas et al., 2008), arriving at the studied locations at 750 m (intermediate boundary layer) and 1500 m (upper boundary layer) Above Ground Level (AGL). PM measurements at the selected background stations show low concentrations of particulates (Table 2) and thus, the trajectory study was focused on 10% of days with highest PM_{10} levels (Engler et al., 2012; Dimitriou and Kassomenos, 2013), in order to identify and analyze atmospheric circulations possibly associated to severe daily events of air quality degradation (Grivas et al., 2008; Kocak et al., 2007). PM_{10} were preferred from $PM_{2.5}$ for this part of the study, due to substantially fewer deficiencies in the data series. The time of every air parcel's arrival in the two cities was set at 12:00 UTC.

The trajectories were then organized in a small number of groups (Dorling et al., 1992; Dorling and Davies, 1995), by an application of a K-means cluster analysis based on the Euclidean distance (Borge et al., 2007; Markou and Kassomenos, 2010). The longitude and latitude of the trajectories over consecutive 1-h intervals were used as clustering variables. Clusters which gathered less that 3% of the total trajectories were rejected as non representative (McGregor, 1993). An average centroid trajectory was computed at each trajectory group, defining the cluster's length and orientation. Haversine formula of the great circle distance between two points was used to define the length (D) of each cluster's centroid trajectory. This length was calculated as the sum of the 96 hourly distances D_i of each pair of neighboring points, along the centroid trajectory (Markou and Kassomenos, 2010), during the 4-day interval. For the needs of this study, trajectory clusters were divided into four main categories, according to the length (D) of their centroid trajectories (Dimitriou and Kassomenos, 2013).

- Short range cluster $0 < D < 1000$ (km)
- Medium range cluster $1000.1 < D < 1800$ (km)
- Long range cluster $1800.1 < D < 3000$ (km)
- Very long range cluster $3000.1 < D$ (km)

The relation of slow moving short range trajectories with the conveyance of PM from transboundary sources, has been revealed in many recent publications (Karaca and Camci, 2010; Salvador et al., 2010; Borge et al., 2007; Makra et al., 2011; Fleming et al., 2012; Udisti et al., 2012; Kassomenos et al., 2012). In short-range transport, the airflow pathway is more influenced by emission source areas than in long range transport, where various exchange and mixing processes (e.g. deposition and advection), physical losses and chemistry have more influence on the composition at the receptor location (Fleming et al., 2012). According to the trajectory analysis conducted by Xu et al. (2006) and Kavouras et al. (2013), the amount of time air spends over a region is linearly related to that region's contribution to pollutants measured at the receptor site. Hence, at all backward atmospheric trajectory clusters in which PM_{10} long range transport impacts were suggested at DEBW081 and DEBB021 sampling sites, residence time of incoming air masses was analyzed on a grid of a $0.5° \times 0.5°$ resolution (Kong et al., 2013), as the sum of the number of trajectory points within each cell. The coordinates of the center of each $0.5° \times 0.5°$ grid cell were used as mapping points, in order to isolate and determine more efficiently, potential external sources of particulates influencing PM_{10} concentrations in Karlsruhe and Potsdam (Chalbot et al., 2013). All the data processing, statistical analysis and graphical representation were performed with SPSS (v.20), Microsoft Excel (v.2007) and R code.

3. Results

3.1. Characterization of PCA results

- **Component 1**: High loadings for CO indicate that this component is strongly affected by traffic emissions (Table 3). During CP, high CO loadings are combined with increased loadings for NO_2, PM_{10} and $PM_{2.5}$, thus the production of particulates is primarily vehicular. Lower loadings for NO_2 at DEBW081 station during CP were considered as a result of simultaneous industrial NO_2 emissions. During WP, PM loadings in Component 1 were significantly reduced (Table 3), hence particulate emissions were no long related to traffic. The decisive drop of PM loadings during WP was detected for both PM_{10} and $PM_{2.5}$, but it was more enhanced for PM_{10} (Table 3), due to the higher dependence of $PM_{2.5}$ emissions by vehicular combustion (Gomes et al., 2008; Kuo et al., 2014). These changes at Component 1 loadings among CP and WP were attributed to reduced traffic flow during WP, as it was indicated by the strongly decreased average daily mean concentrations of CO (Table 2). Thus, Component 1 explained substantially less percentage of the total variance during WP, at both stations (Table 3).
- **Component 2**: During CP and WP, Component 2 is dominated by highly enriched coefficients for O_3 and NO_2, but with opposite signs (Table 3). NO_2 typically arises via the oxidation of Nitric Oxide (NO), which is a well known sink for O_3, thus photochemical air pollution is indicated at both sampling sites.

Table 3
PCA analysis loadings and variance explanation at DEBB021 and DEBW081 stations, during CP and WP separately.

Station	Component	Cold period (CP)				Warm period (WP)			
		1	2	3	4	1	2	3	4
DEBW081 (Karlsruhe-Nordwest)	$PM_{2.5}$	0.872	0.333	0.326	–	0.232	0.347	0.220	0.846
	PM_{10}	0.826	0.310	0.439	–	0.109	0.303	0.190	0.904
	SO_2	0.355	0.258	0.876	–	0.085	0.063	0.952	0.273
	O_3	−0.280	−0.912	−0.231	–	−0.020	0.940	0.042	0.232
	CO	0.591	0.346	0.651	–	0.975	−0.022	0.090	0.200
	NO_2	0.474	0.584	0.493	–	0.231	−0.392	0.428	0.710
	Variance (%)	37.0	26.1	29.8	–	18.0	20.9	19.7	36.8
DEBB021 (Potsdam-Zentrum)	$PM_{2.5}$	0.762	0.045	0.567	–	0.346	0.184	0.326	0.792
	PM_{10}	0.784	0.054	0.535	–	0.095	0.247	.208	0.897
	SO_2	0.266	0.081	0.932	–	.106	0.120	.940	0.293
	O_3	−0.206	−0.960	−0.058	–	−0.262	0.857	0.153	0.370
	CO	0.761	0.407	0.405	–	0.966	−0.071	0.120	0.063
	NO_2	0.849	0.385	0.082	–	0.772	−0.343	0.031	0.385
	Variance (%)	43.5	20.8	27.5	–	29.0	16.1	17.9	30.1

Extraction Method: Principal Component Analysis. Rotation Method: Varimax with Kaiser Normalization.

- **Component 3**: The principal characteristic of Component 3 is the elevated loadings for SO_2 (Table 3), thus this component describes particularly the emissions from industrial (DEBW081) and domestic (DEBB021) activities. Moderate loadings for CO and PM during CP suggest that CO and PM emissions are partially associated with industrial/domestic combustion. The drop of energy consumption during WP provoked a decline of the corresponding at Component 3 percentage of the total variance: [29.8%–19.7%] and [27.5%–17.9%], at DEBW081 and DEBB021 stations respectively (Table 3).
- **Component 4**: This component was computed by PCA analysis only during WP, and reflects the sources of the total production of PM in the selected areas, while less traffic occurs. At the Karlsruhe station (DEBW081), Component 4 was highly enriched by PM_{10}, $PM_{2.5}$ and NO_2 and thus, describes all the combined combustion emissions of particulates from industrial activities and the remaining traffic. At the Potsdam station (DEBB021), Component 4 included very high loadings for PM, moderate loadings for NO_2 and low burden for all the other gaseous pollutants, thus secondary emissions of PM (e.g. natural sources, dust resuspension etc) were more strongly indicated. This component explains a large fraction: 36.8% and 30.1% of the total variance, at DEBW081 and DEBB021 stations respectively (Table 3).

An Independent Variables *T*-Test, revealed a decrease of the $PM_{2.5}/PM_{10}$ fraction during WP, at DEBW081 [6.6% (95% CI: 4.7%, 8.5%)] and DEBB021 [13.6% (95% CI: 11.1%, 16.1%)] stations. The more radical drop in Potsdam was attributed to decreased combustion, in conjunction with the production of more PM_{COARSE} ($PM_{COARSE} = PM_{10}-PM_{2.5}$), due to dust resuspension and biogenic emissions from "Bassiinplatz" park, during summer and spring.

3.2. Characterization of PCC results

PCC were extracted among meteorological parameters (MWS, MWG and RH) and PM_{10} concentrations. Correlations between MWS and PM_{10} were found equal to −0.432 and −0.210, whereas Pearson coefficients calculated among MWG and PM_{10} resulted to be −0.463 and −0.280, in Karlsruhe and Potsdam respectively. These moderate (Karlsruhe) and low-moderate (Potsdam) negative correlations were statistically significant at the 0.01 level and thus, moderate dispersion of particulates due to wind was indentified. PCC among RH and PM_{10} concentrations were considered as too low to be meaningful at both areas (Karlsruhe: 0.035, Potsdam: 0.137), while in Karlsruhe the results were not statistically significant.

3.3. Localization of potential exogenous sources contributing to PM_{10} episodes

- In Karlsruhe, 14 backward trajectory clusters corresponding to increased PM_{10} concentrations were produced [Clusters 1–6 (1500 m AGL), Clusters 7–14 (750 m AGL)]. Clusters 7 and 10 were excluded from the paper [<3%] (Table 4a). At the 1500 m AGL analysis, short range Cluster 4 and medium range Clusters 2 and 5, summarized 33.0%, 22.0% and 23.1% of the total trajectories respectively (Table 4a). At the 750 m AGL analysis, short range Clusters 9 and 12, gathered 27.2% and 28.3% of total trajectories respectively (Table 4b). These high proportions of trajectories classified in short/medium range clusters, indicated associations among the inflow of slow moving air parcels and increased PM_{10} concentrations. In addition, raised average and maximum values of daily mean concentrations of PM_{10} were also calculated in Clusters 2, 4, 5, 9 and 12 (Table 4), and were attributed to the additional quantity of exogenous PM, due to long range transport. Clusters 4 and 12 are consisted from regional all around trajectories originated mainly from Northern Italy, France and Baden Württemberg, where multiple combustion PM sources exist (Fig. 1a). The few trajectories reaching Northern Africa (NA) in Cluster 4 were observed during CP and thus, were not associated with dust transport in Karlsruhe, because Sahara dust outbreak in the Mediterranean and central Europe presents maximum values during spring and summer and minimum values during winter (Athanassiou et al., 2013; Varga et al., 2013). Clusters 5 and 9 include trajectories of continental air masses that approached Karlsruhe from east directions (Fig. 1a). Cluster 2 contains trajectories of air masses that arrived in Karlsruhe from the North, through Germany, Jutland Peninsula and the North Sea (Fig. 1a). In general, low mean wind speeds were calculated at all clusters (Table 4), thus weak dispersion of particulates is suggested.

According to the geographical distribution of the residence time of air masses (Fig. 1 b) approaching the city of Karlsruhe at 750 m AGL, potential transboundary PM sources are localized mainly to the Southwest (Cluster 12) and to the East (Cluster 9) of the city, in France and Germany respectively. Maximum values of air mass residence time are detected in regional areas around the city, and particularly in Baden Württemberg. At Cluster 9, a secondary peak

Table 4
Centroid trajectory length, average daily mean wind speed, number of episodes and PM_{10} concentration statistics, corresponding to backward trajectory clusters at a) 1500 m AGL and b) 750 m AGL.

a) Station	Clusters 1500 m AGL	1	2	3	4	5	6		
DEBW081 (Karlsruhe-Nordwest)	Centroid Length (km)	2898	1544	4980	865	1700	2996	–	–
	PM_{10} Average (ug/m^3)	49.7	52.1	50.3	53.2	52.7	48.0	–	–
	PM_{10} Maximum (ug/m^3)	76	83	72	81	94	62	–	–
	PM_{10} Stan-dev (ug/m^3)	12.5	11.0	12.3	10.1	13.3	7.8	–	–
	PM_{10} Episodes	16	38	7	57	40	15	–	–
	Trajectories (%)	9.2	22.0	4.0	33.0	23.1	8.7	–	–
	Mean wind speed (m/sec)	2.9	2.8	4.1	2.8	3.2	2.8	–	–
DEBB021 (Potsdam-Zentrum)	Centroid Length (km)	1746	1569	2516	2710	4202	769	–	–
	PM_{10} Average (ug/m^3)	64.0	59.0	63.1	66.5	53.7	55.8	–	–
	PM_{10} Maximum (ug/m^3)	158.5	134.7	119.7	143.3	79	192.5	–	–
	PM_{10} Stan-dev (ug/m^3)	32.4	20.7	21.6	24.8	13.2	22.6	–	–
	PM_{10} Episodes	26	39	21	24	8	61	–	–
	Trajectories (%)	14.5	21.8	11.7	13.4	4.5	34.1	–	–
	Mean wind speed (m/sec)	6.4	5.9	6.3	6.6	5.4	5.6	–	–
b) Station	**Clusters 750 m AGL**	**7**	**8**	**9**	**10**	**11**	**12**	**13**	**14**
DEBW081 (Karlsruhe-Nordwest)	Centroid Length (km)		2173	799		1634	589	1979	2063
	PM_{10} Average (ug/m^3)		50.9	54.2		50.8	52.5	50.1	49.0
	PM_{10} Maximum (ug/m^3)		70	94		83	81	66	62
	PM_{10} Stan-dev (ug/m^3)		10.7	13.0		10.9	11.2	8.4	7.7
	PM_{10} Episodes	2	17	47	3	28	49	14	13
	Trajectories (%)	1.2	9.8	27.2	1.7	16.2	28.3	8.1	7.5
	Mean wind speed (m/sec)		4.0	2.7		3.2	2.7	3.1	2.5
DEBB021 (Potsdam-Zentrum)	Centroid Length (km)	1624	2562	515	2885	1743	1091	–	–
	PM_{10} Average (ug/m^3)	59.1	65.0	58.8	67.6	58.7	57.7	–	–
	PM_{10} Maximum (ug/m^3)	192.5	135.9	158.5	143.3	134.6	119.7	–	–
	PM_{10} Stan-dev (ug/m^3)	25.7	31.0	22.1	26.1	25.5	19.7	–	–
	PM_{10} Episodes	56	8	53	19	12	31	–	–
	Trajectories (%)	31.3	4.5	29.6	10.6	6.7	17.3	–	–
	Mean wind speed (m/sec)	5.9	6.5	5.9	6.7	5.9	5.8	–	–

Blank boxes correspond to clusters that include less than 3.0% of the total trajectories and were excluded from the procedure.

of dwelling time density is observed at the intensively industrialized area of Stuttgart, at the East-Southeast of Karlsruhe, and thus an important potential exogenous source of PM is identified. At the 1500 m AGL analysis, increased density of air mass residence time was indicated primarily to the South, mainly over Switzerland (Cluster 4) and up to the borders of industrialized North Italy, and to the East (Cluster 5) over South Germany. In addition, as in the 750 m AGL analysis, highest values of air mass residence time are detected in regional areas around the city.

- In Potsdam, 12 clusters of trajectories associated to elevated PM_{10} levels were created [Clusters 1–6 (1500 m AGL), Clusters 7–12 (750 m AGL)]. At the 1500 m AGL study, short range Cluster 6 and medium range Cluster 2, grouped 34.1% and 21.8% of total trajectories respectively (Table 4a). At the 750 m AGL analysis, medium range Cluster 7 and short range Cluster 9 summarized 31.3% and 29.6% of total trajectories correspondingly (Table 4b). Hence, associations among slow moving air masses and increased PM_{10} levels were suggested. The continental trajectories that were categorized in Clusters 2 and 7, describe the movement of air masses originated from Eastern Europe, whereas Clusters 6 and 9 were consisted by short range all around trajectories that approached Potsdam, mainly through Germany and the Czech Republic. The trajectories that reached NA in Cluster 6 are limited and were observed during CP, hence no Sahara dust intrusion is suggested (Athanassiou et al., 2013; Varga et al., 2013). Higher maximum daily mean PM_{10} concentrations were observed in Clusters 2, 6, 7 and 9. The unexpectedly high average daily mean PM_{10} levels at long range Clusters 3, 4, 8, and 10, which summarized reduced fractions of trajectories (Table 4), were not considered as markers of long range transport contribution and were attributed to enhanced local PM emissions, in conjunction with atmospheric stagnation conditions due to low wind speed (Table 4).

The analysis of air mass residence time revealed elevated dwelling time of incoming air parcels primarily to the south of Potsdam over East and Southeast Germany, the Czech Republic and West Poland. The results were similar at the 1500 m AGL (Cluster 6) and at the 750 m AGL (Cluster 9) analysis (Fig. 2). The so-called European Black Triangle at the Czech-German-Polish border line is included in the area. PM_{10} pollution is believed to be still an actual problem at the Black Triangle, due to coal mining and the presence of large combustion resources (Hykyšová and Brejcha, 2009; Worobiec et al., 2008). At Cluster 2 (1500 m AGL) and primarily Cluster 7 (750 m AGL), enhanced residence time of air parcels approaching Potsdam from East Europe was detected to the Southeast of the city, across Austria and the Czech Republic.

4. Conclusions

The main objective of this paper was to decompose the profile of PM in two low polluted German cities namely: Karlsruhe and Potsdam, focusing on the localization of potential transboundary sources. For this purpose a backward trajectory cluster analysis was implemented, followed by an additional study of air mass residence time on a grid of a 0.5° × 0.5° resolution. In addition, air pollution and meteorological data were inserted to a combination of statistical tools, in order to identify PM emissions in the vicinity of the selected sampling sites.

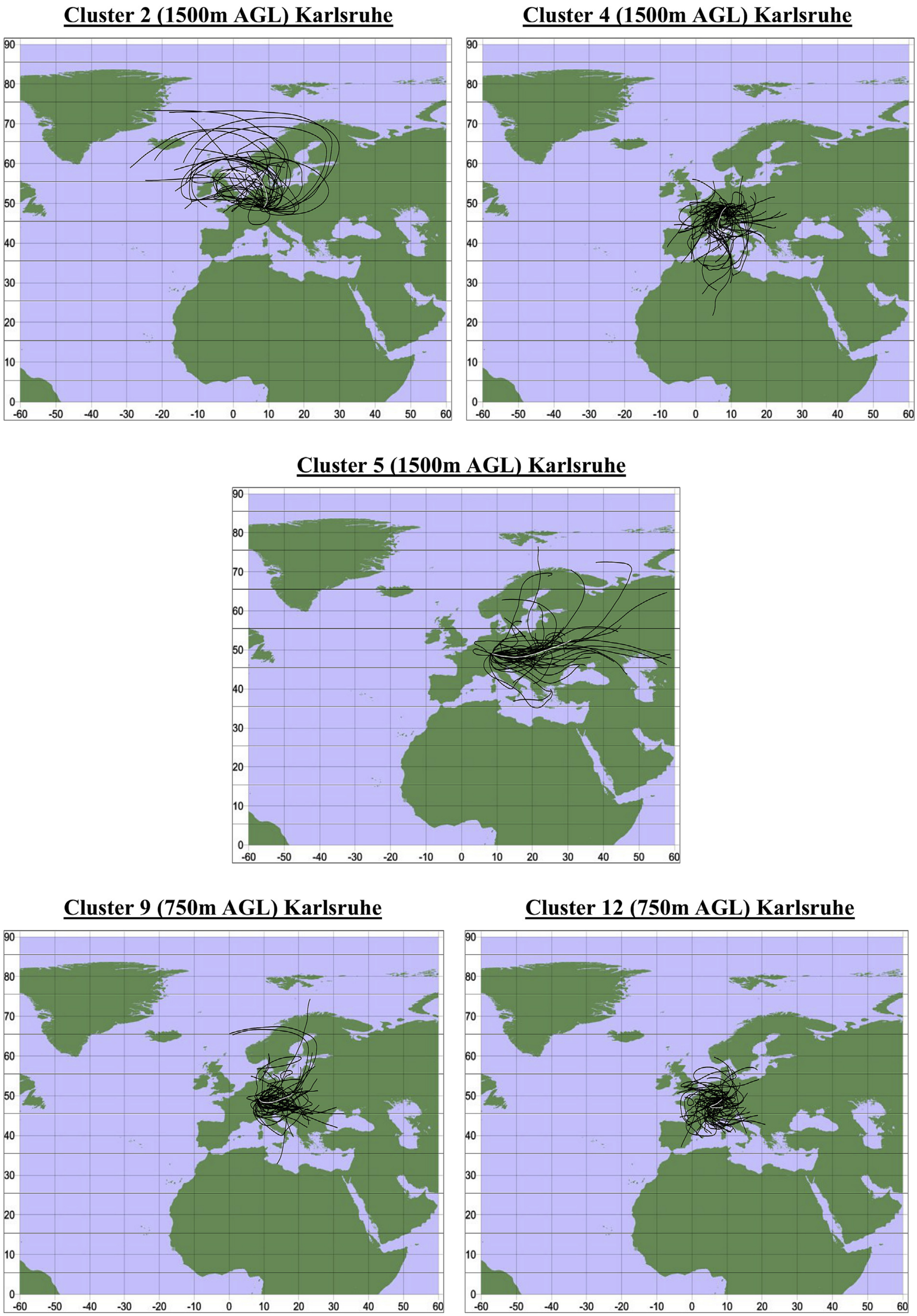

(a)

Fig. 1. a) Trajectory clusters and b) residence time (hours) of air masses, associated with potential PM_{10} transportation in Karlsruhe at 750 m and 1500 m AGL.

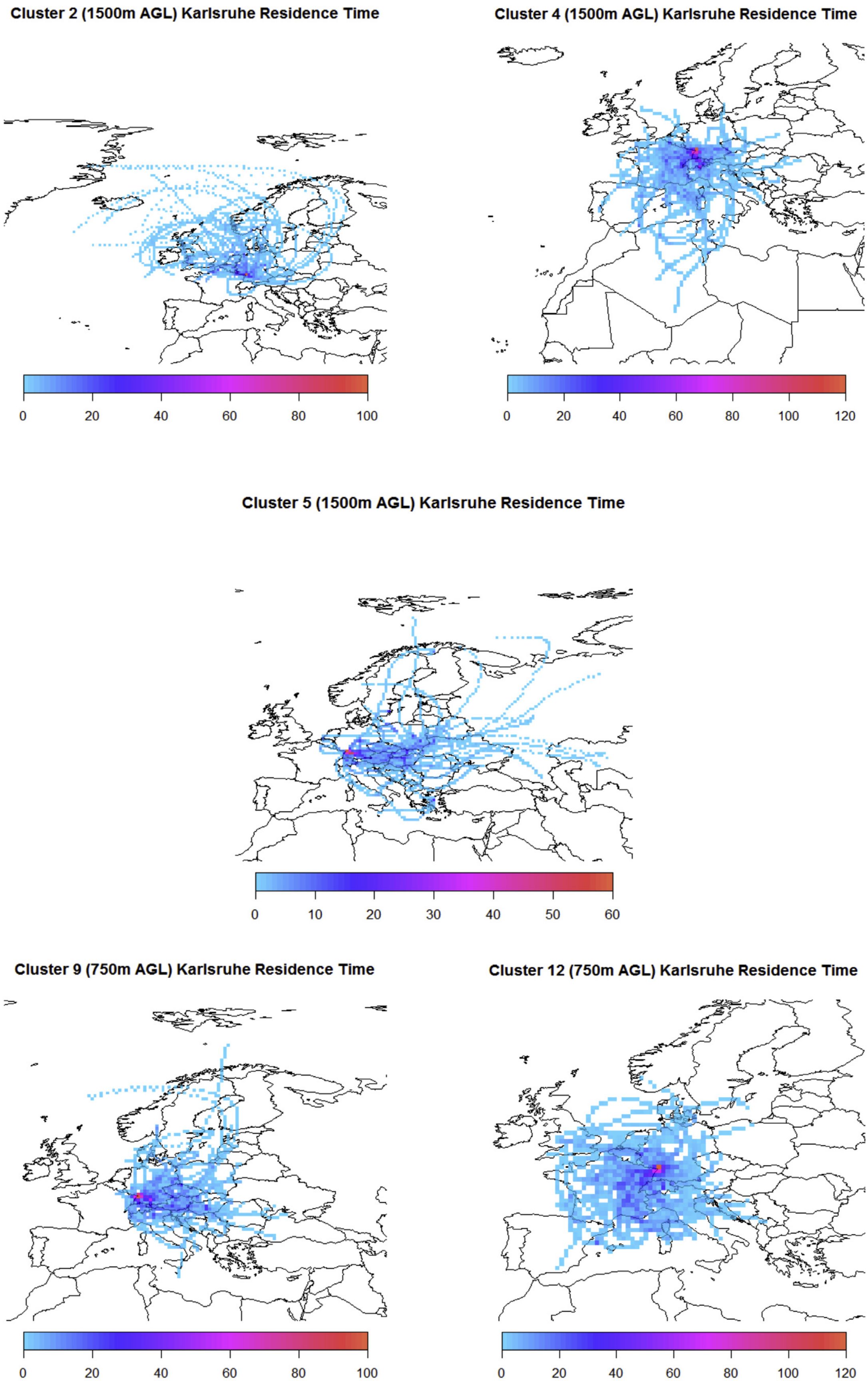

(b)

Fig. 1. (*continued*).

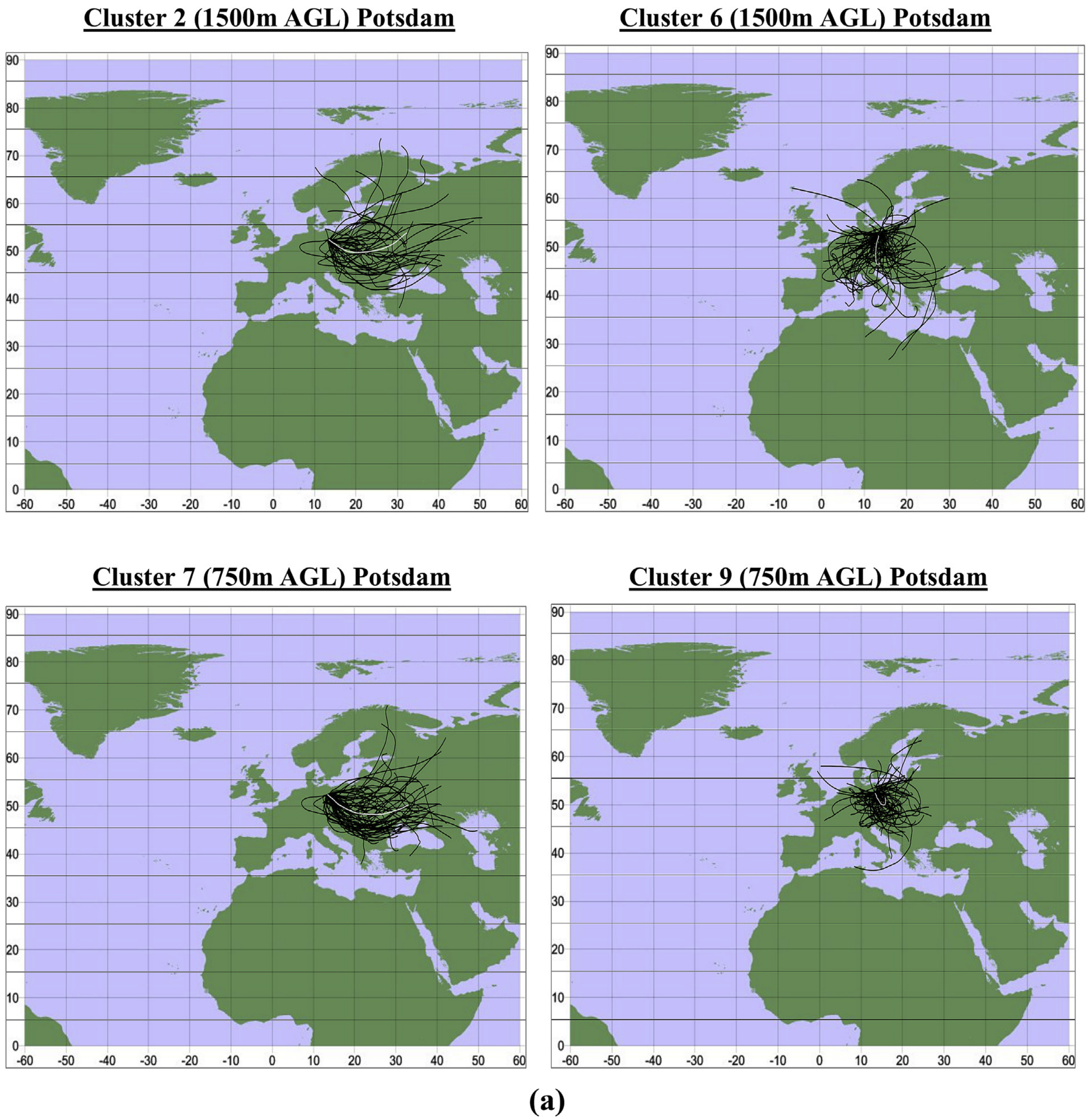

Fig. 2. a) Trajectory clusters and b) residence time (hours) of air masses, associated with potential PM_{10} transportation in Potsdam at 750 m and 1500 m AGL.

The calculation of PCC, between PM_{10} and MWS/MWG, revealed moderate wind dispersion of aerosols at both cities. Daily air pollution data were elaborated by a PCA analysis during CP and WP. PCA produced four air pollution components: Component 1 [traffic], Component 2 [photochemical], Component 3 [industrial/domestic], and Component 4 [particulate]. In the Karlsruhe PCA analysis, Component 4 depicts the total combustion emissions of PM in the area. In the Potsdam PCA analysis, the contribution of secondary PM sources (e.g. natural sources, dust resuspension etc) was indicated. A statistically significant at 95% CI drop in $PM_{2.5}$/PM_{10} values during WP was calculated in Karlsruhe [DEBW081: 6.6% (95% CI: 4.7%, 8.5%)] and Potsdam [DEBB021: 13.6% (95% CI: 11.1%, 16.1%)]. The more radical drop of the proportion $PM_{2.5}$/PM_{10} in Potsdam was attributed to decreased combustion, in conjunction with the production of more PM_{COARSE} from secondary sources. During CP, when Component 4 was not computed, the generation of particles was proven to be primarily vehicular.

Karlsruhe and Potsdam are generally characterized as two low polluted cities and thus, potential particulate intrusions from transboundary sources are critical for the provocation of severe daily PM_{10} episodes, downgrading air quality and health. Short and medium range trajectory clusters, gathered large fractions (Karlsruhe (1500 m AGL): 22.0%–33.0%, Karlsruhe (750 m AGL): 27.2%–28.3%, Potsdam (1500 m AGL): 21.8%–34.1%, Potsdam (750 m AGL): 29.6%–31.3%) of total trajectories corresponding to highest 10% daily mean PM_{10} concentrations and thus, associations among slow moving air masses and increased PM_{10} levels were indicated. Elevated maximum and average daily mean PM_{10} concentrations were calculated at short range clusters affecting Karlsruhe. In Potsdam, peak PM_{10} daily mean concentrations were also detected at short range clusters, whereas high average daily mean PM_{10} levels, observed at long range clusters consisted by reduced fractions (1500 m AGL: 11.7%–14.5%, 750 m AGL: 4.5%–10.6%) of total trajectories, were considered as a result of enhanced local

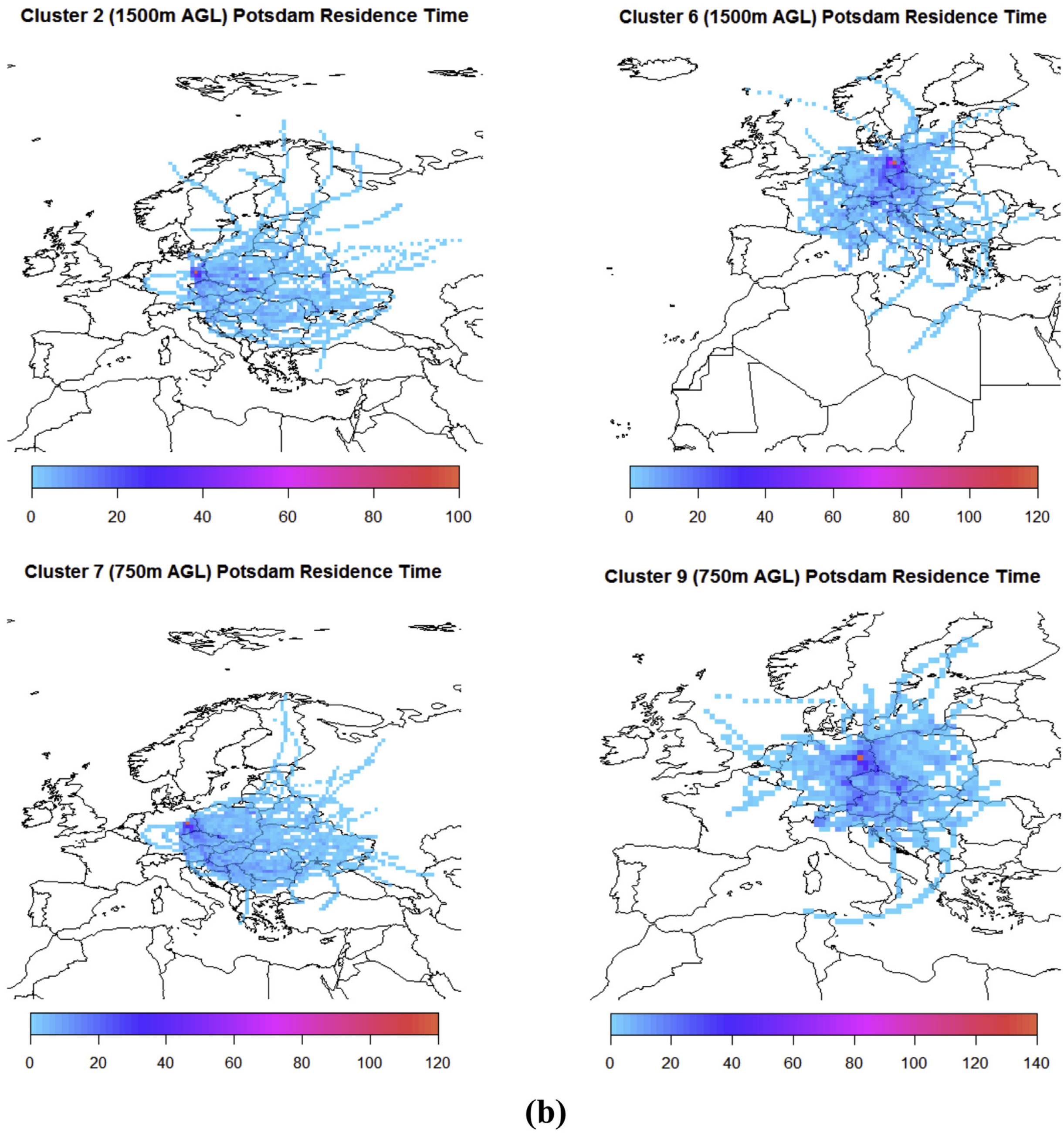

Fig. 2. (*continued*).

emissions, in conjunction with atmospheric stagnation due to low wind. In general, weak wind speeds (2.8 m/sec–6.7 m/s) were calculated in all clusters at both cities.

The residing areas of incoming in Karlsruhe and Potsdam slow moving air masses are potential transboundary sources of PM. For the case of Karlsruhe, those areas were mainly localized in regional terrains around the city, and also in neighboring parts of Germany, France and Switzerland, up to the borders of industrialized North Italy. A secondary peak of residence time was observed over the district of Stuttgart. For the case of Potsdam, areas with increased dwelling time of the arriving air masses were detected particularly above East and Southeast Germany, the Czech Republic and West Poland, where multiple urban and industrial facilities exist. No Sahara dust intrusions were indicated at both cities.

It is a strong belief of the authors that the implemented mixture of methods achieved the goals of this paper. Nevertheless, further research and discussion is needed on this matter, primarily in the field of long range transport. An analysis of PM chemical properties at the receptor sites could provide beneficial information and expand the findings of this paper.

Acknowledgments

The authors would like to thank the European Union (EU) Air Quality Database (Airbase), for the provision of air pollution data, and also the European Climate Assessment & Dataset (ECA&D) project, for the concession of meteorological data. We would also like to acknowledge the contribution of the NOAA Air Resources

Laboratory, for the kind and unrestricted provision of the HYSPLIT trajectory model.

References

Athanassiou, G., Hatzianastassiou, N., Gkikas, A., Papadimas, C.D., 2013. Estimating aerosol optical depth over the broader greek area from MODIS satellite. Water Air Soil. Pollut. 224 (7). http://dx.doi.org/10.1007/s11270-013-1605-2. Article number 1605.

Borbely-Kiss, I., Koltay, E., Szabo, G.Y., Bozo, L., Tar, K., 1999. Composition and sources of urban and rural atmospheric aerosol in eastern Hungary. J. Aerosol Sci. 30 (3), 369–391.

Borge, R., Lumbreras, J., Vardoulakis, S., Kassomenos, P., Rodriguez, E., 2007. Analysis of long range transport influences on urban PM_{10} using two-stage atmospheric trajectory clusters. Atmos. Environ. 41, 4434–4450.

Chalbot, M.-C., Lianou, M., Vei, I.-C., Kotronarou, A., Kavouras, I.G., 2013. Spatial attribution of sulfate and dust aerosol sources in an urban area using receptor modeling coupled with Lagrangian trajectories. Atmos. Poll. Res. 4, 346–353.

Chaloulakou, A., Kassomenos, P., Spyrellis, N., Demokritou, P., Koutrakis, P., 2003. Measurements of PM10 and PM2.5 particle concentrations in Athens, Greece. Atmos. Environ. 37, 649–660.

Charron, A., Harrison, R., Quincey, P., 2007. What are the sources and conditions responsible for exceedences of the 24 h PM10 limit value (50 mgm_3) at a heavily trafficked London site? Atmos. Environ. 41, 1960–1975.

Chen, R., Chu, C., Tan, J., Cao, J., Song, W., Xu, X., Jiang, C., Ma, W., Yang, C., Chen, B., Gui, Y., Kan, H., 2010. Ambient air pollution and hospital admission in Shanghai, China. J. Hazard Mater. 181, 234–240.

Deacon, A.R., Derwent, R.G., Harrison, R.M., Middleton, D.R., Moorcroft, S., 1997. Analysis and interpretation of measurements of suspended particulate matter at urban background sites in the United Kingdom. Sci. Total Environ. 203, 17–36.

Demirci, E., Cuhadaroglou, B., 2000. Statistical analysis of wind circulation and air pollution in urban Trabzon. Energy Build. 31, 49–53.

Dimitriou, K., Kassomenos, P.A., 2013. The fine and coarse particulate matter at four major Mediterranean cities: local and regional sources. Theor. Appl. Clim. 114, 375–391. http://dx.doi.org/10.1007/s00704-013-0851-y.

Dorling, S.R., Davies, T.D., Pierce, C.E., 1992. Cluster Analysis: a technique for estimating the synoptic meteorological controls on air and precipitation chemistry-method and applications. Atmos. Environ. 26, 2575–2581.

Dorling, S.R., Davies, T.D., 1995. Extending cluster analysis-synoptic meteorology links to characterise chemical climates at six northwest European monitoring stations. Atmos. Environ. 29, 145–167.

Engler, C., Birmili, G., Spindler, G., Wiedensohler, A., 2012. Analysis of exceedances in the daily PM10 mass concentration (50 μgm^{-3}) at a roadside station in Leipzig, Germany. Atmos. Chem. Phys. 12, 10107–10123.

Fleming, Z.L., Monks, P.S., Manning, A.J., 2012. Review: untangling the influence of air-mass history in interpreting observed atmospheric composition. Atmos. Res. 104–105, 1–39.

Gehrig, R., Buchmann, B., 2003. Characterising seasonal variations and spatial distribution of ambient PM10 and PM2.5 concentrations based on long-term Swiss monitoring data. Atmos. Environ. 37, 2571–2580.

Gomes, L., Mallet, M., Roger, J.C., Dubuisson, P., 2008. Effects of the physical and optical prosperities of urban aerosols measured during the CAPITOUL summer campaign on the local direct radiative forcing. Meteorol. Atmos. Phys. 102, 289–306.

Grivas, G., Chaloulakou, A., Kassomenos, P., 2008. An overview of the PM10 pollution problem, in the Metropolitan Area of Athens, Greece. Assessment of controlling factors and potential impact of long range transport. Sci. Total Environ. 389, 165–177.

Guo, Y., Tong, S., Zhang, Y., Barnett, A.G., Jia, Y., Pan, X., 2010. The relationship between particulate air pollution and emergency hospital visits for hypertension in Beijing, China. Sci.Total Environ. 408, 4446–4450.

Gupta, A.K., Patil, R.S., Gupta, S.K., 2004. Influence of meteorological factors on air pollution concentration for a coastal region in India. Int. J. Environ. Poll. 21, 253–262.

Hykyšová, S., Brejcha, J., 2009. Monitoring of PM10 air pollution in small settlements close to opencast mines in the North-Bohemian Brown Coal Basin. WIT. Trans. Ecol. Environ. 123, 387–398.

Jiménez, E., Linares, C., Rodríguez, L.F., Bleda, M.J., Díaz, J., 2009. Short-term impact of particulate matter (PM2.5) on daily mortality among the over-75 age group in Madrid, Spain. Sci. Total Environ. 407, 5486–5492.

Jiménez, E., Linares, C., Martínez, D., Díaz, J., 2010. Role of Saharan dust in the relationship between particulate matter and short-term daily mortality among the elderly in Madrid, Spain. Sci. Total Environ. 408, 5729–5736.

Karaca, F., Anil, I., Alagha, O., 2009. Long-range potential source contributions of episodic aerosol events to PM_{10} profile of a megacity. Atmos. Environ. 43, 5713–5722.

Karaca, F., Camci, F., 2010. Distant source contributions to PM_{10} profile evaluated by SOM based cluster analysis of air mass trajectory sets. Atmos. Environ. 44, 892–899.

Kassomenos, P., Vardoulakis, S., Chaloulakou, A., Grivas, G., Borge, R., Lumbreras, J., 2012. Levels, sources and seasonality of coarse particles (PM10-PM2.5) in three European capitals – implications for particulate pollution control. Atmos. Environ. 54, 337–347.

Kavouras, I.G., Lianou, M., Chalbot, M.-C., Vei, I.C., Kotronarou, A., Hoek, G., Hameri, K., Harrison, R.M., 2013. Quantitative determination of regional contributions to fine and coarse particle mass in urban receptor sites. Environ. Poll. 176, 1–9.

Kocak, M., Mihalopoulos, N., Kubilay, N., 2007. Contributions of natural sources to high PM_{10} and $PM_{2.5}$ events in the eastern Mediterranean. Atmos. Environ. 41, 3806–3818.

Kong, X., He, W., Qin, N., He, Q., Yang, B., Ouyang, H., Wang, Q., Xu, F., 2013. Comparison of transport pathways and potential sources of PM10 in two cities around a large Chinese lake using the modified trajectory analysis. Atmos. Res. 122, 284–297.

Kuo, C.P., Liao, H.T., Chou, C.C.-K., Wu, C.F., 2014. Source apportionment of particulate matter and selected volatile organic compounds with multiple time resolution data. Sci. Total Environ. 472, 880–887.

Lewandowska, A., Falkowska, L., Joswik, J., 2013. Factors determining the fluctuation of fluoride concentrations in PM10 aerosols in the urbanized coastal area of the Baltic Sea (Gdynia, Poland). Environ. Sci. Pollut. Res. 20, 6109–6118.

Linares, C., Diaz, J., 2010. Short-term effect of concentrations of fine particulate matter on hospital admissions due to cardiovascular and respiratory causes among the over-75 age group in Madrid, Spain. Public Health 124, 28–36.

Makra, L., Matyasovszky, I., Guba, Z., Karatzas, K., Anttila, P., 2011. Monitoring the long-range transport effects on urban PM_{10} levels using 3D clusters of backward trajectories. Atmos. Environ. 45, 2630–2641.

Markou, M., Kassomenos, P., 2010. Cluster analysis of five years of back trajectories arriving in Athens, Greece. Atmos. Res. 98, 438–457.

McGregor, G.R., 1993. A multivariate approach to the climatic region and climatic resources of China. Geoforum 24, 357–380.

Minguillon, M.C., Monfort, E., Escrig, A., Celades, I., Guerra, L., Busani, G., Sterni, A., Querol, X., 2013. Air quality comparison between two European ceramic tile clusters. Atmos. Environ. 74, 311–319.

Mirante, F., Salvador, P., Pio, C., Alves, C., Artiñano, B., Caseiro, A., Revuelta, M.A., 2014. Size fractionated aerosol composition at roadside and background environments in the Madrid urban atmosphere. Atmos. Res. 138, 278–292.

Norra, S., Stuben, D., 2004. Trace element patterns and seasonal variability of dust precipitation in a low polluted city – the example of Karlsruhe/Germany. Environ. Monit. Assess. 93, 203–228.

Oguz, E., Kava, M.D., Nuhoglu, Y., 2003. Interaction between air pollution meteorological parameters in Erzurum, Turkey. Int. J. Environ. Poll. 19, 292–300.

Polissar, A.V., Hopke, P.K., Poirot, R.L., 2001. Atmospheric aerosol over Vermont: chemical composition and sources. Environ. Sci. Technol. 35, 4604–4621.

Riccio, A., Giunta, G., Chianese, E., 2007. The application of a trajectory classification procedure to interpret air pollution measurements in the urban area of Naples. Sci. Total Environ. 376, 198–214.

Salvador, P., Artinano, B., Pio, C., Afonso, J., Legrand, M., Puxbaum, H., Hammer, S., 2010. Evaluation of aerosol sources at European high altitude background sites with trajectory statistical methods. Atmos. Environ. 44, 2316–2329.

Sarkar, S., Khillare, P.S., 2013. Profile of PAH_S in the inhalable particulate fraction: source apportionment and associated health risks in a tropical megacity. Environ. Monit. Assess. 185 (2), 1199–1213.

Tabaku, A., Bejtja, G., Bala, S., Toci, E., Resuli, J., 2011. Effects of air pollution on children's pulmonary health. Atmos. Environ. 45, 7540–7545.

Udisti, R., Dayan, U., Becagli, S., Busetto, M., Frosini, D., Legrand, M., Lucarelli, F., Preunkert, S., Severi, M., Traversi, R., Vitale, V., 2012. Sea spray aerosol in central Antarctica. Present atmospheric behaviour and implications for paleoclimatic reconstructions. Atmos. Environ. 52, 109–120.

Varga, G., Kovacs, J., Ujvari, G., 2013. Analysis of Saharan dust intrusions into the Carpathian Basin (Central Europe) over the period of 1979–2011. Glob. Planet. Change 100, 333–342.

Vardoulakis, S., Kassomenos, P., 2008. Sources and factors affecting PM_{10} levels in two European cities: Implications for local air quality management. Atmos. Environ. 42, 3949–3963.

Viana, M., Pey, J., Querol, X., Alastuey, A., de Leeuw, F., Lükewille, A., 2014. Natural sources of atmospheric aerosols influencing air quality across Europe. Sci. Total Environ. 472, 825–833.

Worobiec, A., Zwozdziak, A., Sowka, I., Zwozdziak, J., Stefaniak, E.A., Buczynska, A., Krata, A., Van Meel, K., Van Grieken, R., Gorka, M., Jedrysek, M.O., 2008. Historical changes in air pollution in the tri-border region of Poland, Czech Republic and Germany. Environ. Prot. Eng. 34 (4), 81–90.

Xu, J., DuBois, D., Pitchford, M., Green, M., Etyemezian, V., 2006. Attribution of sulfate aerosols in Federal Class I areas of the western United States based on trajectory regression analysis. Atmos. Environ. 40, 3433–3447.

Yoo, H.J., Kim, J., Muk, Yi.S., Duk, Zoh.K., 2011. Analysis of black carbon, particulate matter, and gaseous pollutants in an industrial area in Korea. Atmos. Environ. 45, 7698–7704.

Zhu, Z., Sun, G., Bi, X., Li, Z., Yu, G., 2013. Identification of trace metal pollution in urban dust from kindergartens using magnetic, geochemical and lead isotopic analyses. Atmos. Environ. 77, 9–15.